The role of excited H_2 in protoplanetary disks

Sietske Bouma
Supervisor: Inga Kamp

July 24, 2014

Abstract

This thesis discusses how much influence excited H_2 has on different molecular species in the protoplanetary disk. Since H_2 contains more energy in its excited state than in its ground state, some reactions that have an activation barrier or are endothermic, can proceed faster with excited H_2. The extra energy is used to overcome the barrier.
Also, the reaction rate for the reaction $H_2(v = 1) + C^+ \rightarrow CH^+ + H$ is discussed. An Arrhenius equation is used to fit the reaction rate. The ProDiMo code from Woitke et al. (2009) was used to model class II protoplanetary disks surrounding low mass stars.
Besides a standard model, four other models were used, one without excited H_2, one with an adjusted reaction rate for $H_2(v = 1) + C^+$, another one had an increased UV flux and the last one was a model of a Herbig Ae/Be star. The masses and the line fluxes of different species were compared in the different models. The influence of excited H_2 on CH^+ and indirect on HCO^+ is especially important in this thesis. Boltzmann plots were made for rotational emission lines of CH^+ and the rotational temperature was derived from them. This was compared to an observed rotational temperature for CH^+.
It can be concluded that excited H_2 has the largest influence on CH^+ and HCO^+. In the absence of excited H_2, the low rotational lines of CH^+ decreased more in flux than the higher rotational lines. The difference for the low lines should be detectable. For HCO^+ the decrease in line flux is probably too small to be detected.
If the UV flux was increased, the masses of CH^+ and HCO^+ became higher, just as their line fluxes. For the Herbig Ae/Be star, this also happened, but the increase was less than with the increased UV flux.

Contents

1 Introduction **2**
- 1.1 Properties of protoplanetary disks . . . 2
- 1.2 Formation and excitation of H_2 in the ISM . . . 3

2 Excited H_2 modelled by ProDiMo **5**
- 2.1 Location of excited H_2 . . . 7
- 2.2 Reactions of excited H_2 . . . 9
- 2.3 Reaction rate for H_2(v=1) + C^+ . . . 12

3 Comparison of physical quantities **14**
- 3.1 Excited H_2 . . . 16
- 3.2 CH^+ . . . 16
- 3.3 He . . . 18
- 3.4 OH . . . 19
- 3.5 H_2O . . . 21
- 3.6 HCO^+ . . . 21

4 Comparison of observable quantities **24**
- 4.1 CH^+ . . . 24
- 4.2 OH and H_2O . . . 26
- 4.3 HCO^+ . . . 26
- 4.4 Boltzmann plots . . . 26

5 Comparison results from ProDiMo with results from real objects **29**

6 Conclusion **31**

7 Acknowledgements **32**

8 References **33**

1 Introduction

The most abundant gas in the universe is H_2. It plays an important role in all kinds of processes. It is the main component in the molecular clouds that are home to star formation. Likewise, it is an important molecule in the protoplanetary disk that is formed around a young star. A protoplanetary disk is formed when a protostar accretes material from the surrounding envelope. This accretion from the disk occurs between 1 and 10 Myr (Muzerolle et al. 2000). The material that surrounds the star cannot fall directly into the star, because it has a certain amount of angular momentum. It forms a disk, from which angular momentum is transported towards the outer part, thus allowing the inner part to loose angular momentum and fall into the central star. Angular momentum is absorbed by part of the mass, which flows outward (Lynden-Bell and Pringle, 1974).

There are several stages in which a dense, molecular cloud becomes a star. These stages are characterised by different spectral energy distributions (SEDs). The first stage in this process is a star with a protoplanetary disk that have an SED of class 0. In this stage the star is surrounded by an envelope and it has a bipolar outflow.

After this, the star accretes from the disk while the disk accretes from the remaining envelope, its SED is now class I. Bipolar outflow still exist, but this outflow is less than before. Also, the mass accretion rate has decreased by a factor 5-10 compared to class 0 (Andre et al., 1999).

When the star and disk become of class II the bipolar outflow and envelope no longer exist, only the disk around the star remains (Ryan and Norton, 2010). This thesis will be about stars with an SED of class II.

First, some general properties of protoplanetary disks and formation of excited H_2 will be discussed, then the code used for modelling excited H_2 in protoplanetary disks will be introduced. Several reactions of excited H_2 are also mentioned in that section, one of them will be discussed in detail. After that the physical and observable quantities of different models will be compared. Finally, a comparison of one of the models with an observed object will be given.

1.1 Properties of protoplanetary disks

The envelope around a star is gone when the SED of the star and the disk is of class II, so observations are no longer obstructed by this envelope. The protostar and its disk can be observed. Protoplanetary disks are disks around young stars and are composed of gas and dust. The disk absorbs light from the central star and emits it again, but at a longer wavelength. This causes reddening of the star. The amount of infrared excess observed from young stars indicates a disk with a flaring shape and not a flat disk (Kenyon and Hartmann, 1987). In a flat disk, the part close to the star would absorb the light and the part farther away would not be able to absorb that much light. The amount of infrared excess this would cause, calculated by Adams et al. (1987) is not enough to explain how much we observe (Rydgren and Zak, 1987). If the disk has a flared shape, the part of the disk that is farther from the star, can still intercept starlight at its surface. This will cause the entire surface to heat and re-emit the light, instead of only a part of the disk close to the star.

The upper layer of a protoplanetary disk differs from the midplane in composition and temperature. Radiation from the central star is absorbed by dust grains in the surface layer and emitted again as thermal radiation, which heats the midplane (Calvet, 1992). Thus, the surface layer is warmer than the midplane, except for radii smaller than a few AU, where heating from mass accretion plays a role (Bergin et al. 2007). Since temperature increases with scale height

of the disk at radii larger than a few AU, the gas will go from molecular to atomic and even to ionized as you go from the midplane to the surface (Williams and Cieza, 2011). The surface of the disk is a photon-dominated region (PDR), there is UV radiation from the central star and also radiation from the interstellar radiation field. The photon energy is high and chemical bonds can be broken, this is photodissociation (Shaw, 2006). Chemistry cannot happen here, since photolysis destroys molecules. Another process that occurs due to this radiation is photoionisation, in which an electron is removed from a molecule or an atom.

In the part between the midplane and the surface layer,the temperature is several tens of Kelvins and the density is high enough ($> 10^6$ cm^{-3}) for molecules to survive (Bergin et al. 2007). In this layer chemistry is possible.

The temperature in the midplane is lower than the freeze-out temperature of CO ($\sim$ 20 K) and heavy-element species form ices on dust grains (Bergin et al. 2007) Small dust particles are distributed throughout the gas, but as they collide and grow, they tend to settle towards the midplane (Dubrulle et al. 1995). The core of dust grains consists of silicates, such as olivine (Draine, 2003). Icy mantles made of H_2O, CO, NH_3 and other species form around these cores. The gas in the midplane is depleted from these species. Because there is photodissociation at the surface and adsorption onto dust grains in the midplane, the molecule abundance is highest in the area in between (Aikawa and Herbst, 1999).

By observing thermal emission of dust, it is found that the temperature not only decreases as one goes from the surface layer to the midplane, it also decreases with radius: T α r^{-q} where q = 0.5-0.75 (Bergin et al. 2007 and references therein). The surface density also decreases with radius:Σ α r^{-p} where p = 0-1 . A lot of chemical reactions depend on temperature, one of them is analysed in Sect. 2.3. But before going into reactions with excited H_2, the formation of excited H_2 will be dicussed.

1.2 Formation and excitation of H_2 in the ISM

The primary gaseous species in protoplanetary disks is H_2. It can be formed by gas phase reactions, but the catalysis by dust grains is much more efficient. The reason for this is that when a new molecule is formed due to the collision of two atoms, there is also energy released by the formation of the new chemical bond. This energy needs to be dissipated, otherwise the molecule will dissociate. A way to get rid of the energy is by radiation, but because H_2 has no dipole moment, there are no allowed dipole transitions (Shaw, 2006).

Formation of H_2 on dust grains happens as follows. An H atom can collide with a dust particle and stick to the surface of the grain. It has some ability to move, so it can collide with another H atom on the surface. The reaction gives an H_2 molecule and energy. The energy is due to formation of the bond between the atoms and one-third of this energy is absorbed by the grain (Shaw, 2006). Another third goes into kinetic energy of H_2 and the last part goed into excitation. H_2 is then freed from the grain and becomes part of the gas.

H_2 can be vibrationally excited by intense ultraviolet (UV) radiation. This is generated for example by accretion of mass onto the star and a PDR is formed because of this radiation (Habart et al. 2005). The UV radiation pumps the H_2 molecule to an electronically excited state. In this state, an electron has gained energy from the photon, but is still bound. The molecule will go back to its electronic ground state and by going through different vibrational levels, it will also, eventually, reach its vibrational ground state. Optical and infrared emission will be emitted due to this cascade to v = 0. In a protoplanetary disk, this process occurs

mostly at the surface layers, because that is where UV radiation can reach H_2. Apart from electronic and vibrational excitation, H_2 can also be rotationally excited. Each vibrational level is split up into multiple rotational levels. Fig. 1 illustrates this.

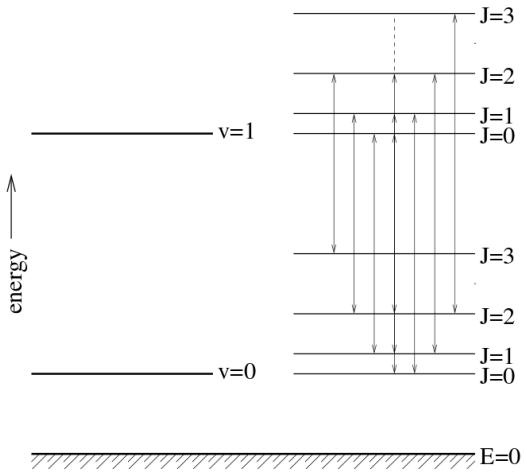

Figure 1: *Energy levels of H_2. The v levels are the vibrational levels and J levels are the rotational levels. Not all energy levels are included. Arrows indicate possible transitions. Fig. from: home.strw.leidenuniv.nl/∼ michiel/ismclass_files/radproc07/chapter8.pdf*

Since excited H_2 has more energy than ground state H_2, some reactions will procede faster with excited H_2.

A typical two-body reaction goes like this:

$$A + B \rightarrow C + D$$

This procedes at a certain rate, the reaction rate. The reaction rate depends on the concentration of both reacting species and on a rate constant (Shaw, 2006).
$r = k[A]^a[B]^b$
r is the reaction rate, k is the rate constant and [A] and [B] are the concentrations of the species A and B respectively. The rate constant can usually be described by an Arrhenius equation. An Arrhenius reaction has the following form:

$$k(T) = Ae^{-E_a/RT}$$

Where A is the total number of collisions per second, which depends on the cross section of the species. A should have the same units as k. E_a is the activation energy, R the ideal gas constant and T the temperature. This equation can be modified to:

$$k(T) = A\ (T/300)^B e^{-C/T}$$

A is the collisional cross section, the factor $(T/300)^B$ has to do with the thermal velocity component of the species that collide. The exponential term takes a possible activation barrier into account. This form will be used later.

2 Excited H_2 modelled by ProDiMo

The ProDiMO code models a young star with a protoplanetary disk around it. The physical and chemical structure of the protoplanetary disk is calculated. A network of chemical reactions is used to model the disk. Different parameters of the star and the disk can be adjusted just as the reactions that occur in the disk. The parameters used in the standard model are listed in Table 1. These parameters determine the physical properties of the disk such as flaring and they influence the chemical reactions that occur in the disk.
The output includes plots that show abundances of different species through the disk, as well as gas and dust temperatures and heating and cooling mechanisms.

Table 1: Parameters of the standard model

Parameter	**Value**
Stellar mass	0.7 $M_\odot$
Stellar luminosity	1.0 $L_\odot$
Stellar effective temperature	4000.0 K
fUV (L_{UV}/L_{star})	0.01
pUV	1.0
Disk mass	0.01 $M_\odot$
Dust-to-gas mass ratio	0.01
Mass density dust grain material	2.094 g/cm^3
Minimum dust particle size	0.05 μm
Maximum dust particle size	3000.0 μm
Inner disk radius	0.07 AU
Outer disk radius	400.0 AU

We assumed a star that had a mass of 0.7 $M_\odot$, an effective temperature of 4000 K and solar luminosity. The luminosity of the star in the UV divided by the total luminosity is called fUV. This is assumed to be 0.01. This means that there is an excess of luminosity in the UV with respect to a stellar model at 4000 K. The flux in the UV is proportional to its wavelength:

$$F_{UV} \propto \lambda^{pUV}$$

In the standard model pUV = 1. Fig. 2 shows how this UV excess is visible when the stellar atmosphere model is plotted together with a blackbody of the same temperature.

The UV part of the spectrum of the star shows a straight line, which is higher than the blackbody spectrum. Since UV radiation is at a short wavelength (912 - 2600 Å, or 92.1 - 260 nm), each photon has a large energy. Due to the flaring shape, the UV radiation can reach the surface of the disk even at large distance. At the surface layer photoionisation and photodissociation take place.

The elements and other species that are included in the standard model are listed in Table 2.

The density structure of the disk is shown in Fig. 3, and the temperature structure is in Fig. 4. The x-axis represents the radius of the disk, while the y-axis shows the height above the midplane, divided by the radius. Gas temperature ranges from less than 10 Kelvin in the midplane at more than 100 astronomical units (AU) from the star, to about 5000 K at the surface of the disk. The gas cools rapidly when going from the surface to the midplane.
The density falls of with radius, just as the surface density which was discussed in Sect. 1.1. The extinction in the V band (A_V) is shown by the dashed lines.

Table 2: Standard selection of elements and chemical (gas + ice) species. Stable species are indicated in bold font.

12 elements	H, He, C, N, O, Ne, Na, Mg, Si, S, Ar, Fe	
(H)	H, H^+, H^-, $\mathbf{H_2}$, H_2^+, H_3^+, H_2^{exc}	7
(He)	He, He^+,	2
(C-H)	C, C^+, C^{++}, CH, CH^+, CH_2, CH_2^+, CH_3, CH_3^+, $\mathbf{CH_4}$, CH_4^+, CH_5^+,	12
(C-N)	CN, CN^+, **HCN**, HCN^+, $HCNH^+$	5
(C-O)	**CO**, CO^+, HCO, HCO^+, $\mathbf{CO_2}$, CO_2^+, HCO_2^+,	7
(N-H)	N, N^+, N^{++}, NH, NH^+, NH_2, NH_2^+, $\mathbf{NH_3}$, NH_3^+, NH_4^+	9
(N-N)	$\mathbf{N_2}$, N_2^+, HN_2^+,	3
(N-O)	NO, NO^+,	2
(O-H)	O, O^+, O^{++}, OH, OH^+, $\mathbf{H_2O}$, H_2O^+, H_3O^+,	8
(O-O)	$\mathbf{O_2}$, O_2^+,	2
(O-S)	SO, SO^+, $\mathbf{SO_2}$, SO_2^+, HSO_2^+	5
(S-H)	S, S^+, S^{++},	3
(Si-H)	Si, Si^+, Si^{++}, SiH, SiH^+, SiH_2^+,	6
(Si-O)	**SiO**, SiO^+, $SiOH^+$,	3
(Na)	Na, Na^+, Na^{++},	3
(Mg)	Mg, Mg^+, Mg^{++},	3
(Fe)	Fe, Fe^+, Fe^{++},	3
(Ne)	Ne, Ne^+, Ne^{++},	3
(Ar)	Ar, Ar^+, Ar^{++},	3
ice	CO#, H_2O#, CO_2#, CH_4#, NH_3#, SiO#, SO_2#, O_2#, HCN#, N_2#	10
species	total	100

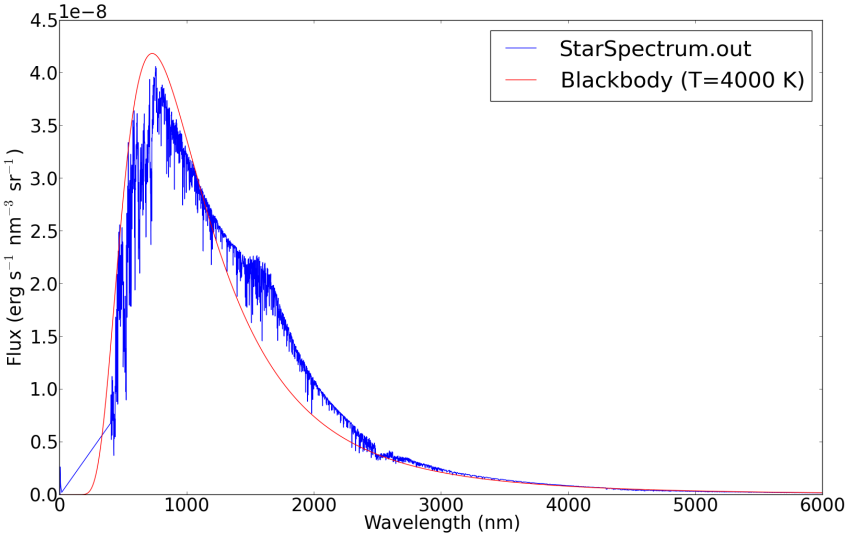

Figure 2: *Spectrum of the standard model from ProDiMo and a blackbody spectrum*

As said before, ProDiMo gives as output also plots of abundances of species. One of these plots shows the abundance of excited H_2. The location and reactions with excited H_2 will be discussed next.

2.1 Location of excited H_2

The only excited level of H_2 that is included in the chemistry of ProDiMo is the first vibrational level, v = 1. In this level H_2 is assumed to be in the rotational ground state.

When running the standard model, that was described before, the total mass of the disk is: 0.01 $M_\odot$ The mass of excited H_2 is $4.4 \cdot 10^{-11}$ $M_\odot$. Only a small fraction, 6 $\cdot 10^{-6}$ permille, of the H_2 is excited, since the mass of H_2 in the ground state is $7.1 \cdot 10^{-3}$ $M_\odot$.

Fig. 5 shows the abundance of excited H_2 in the protoplanetary disk. Most excited H_2 is located at the surface layer, and in the flaring outer part. As said before, this is where the light of the central star can reach the H_2 to excite it.

$$H_2 + \text{photon} \rightarrow H_2(v = 1) \tag{1}$$

UV light is not the only mechanism to bring H_2 in an excited state, the following collisional reaction also has that effect:

$$H_2 + H_2 \rightarrow H_2(v = 1) + H_2 \tag{2}$$

In this reaction a part of the kinetic energy is transferred to one of the H_2 molecule, thereby exciting it. In Fig. 6 you can see where which process is the primary process to excite H_2.

From this plot, it is observed that most formation in the upper layer is due to starlight, while there is a diagonal area deeper into the disk, where reaction (2) is the main formation reaction.

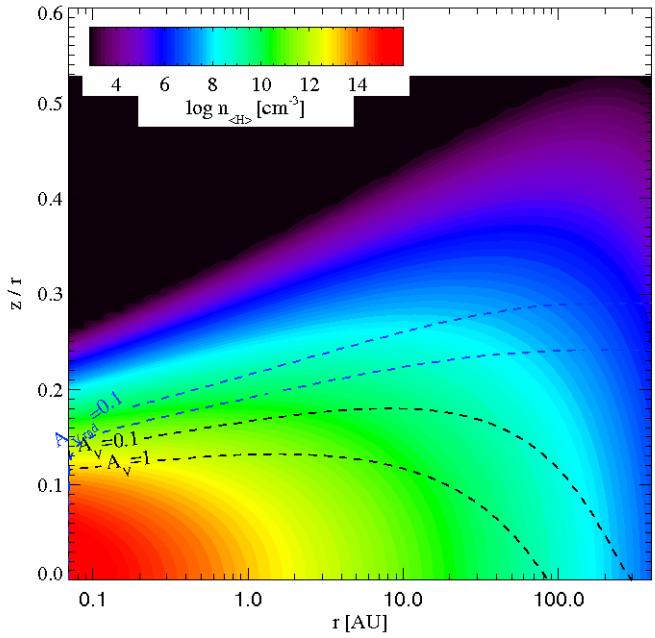

Figure 3: *Density in the standard model. Blue dashed lines give the radial extinction in the V band, white dashed lines the exctinction in the V band.*

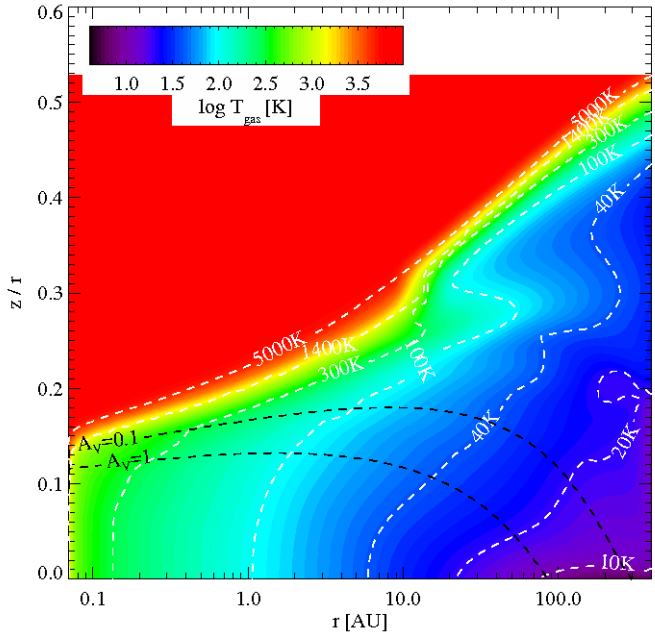

Figure 4: *Temperature of the gas in the standard model. White dashed lines are isotherms, black dashed lines give the extinction in the V band.*

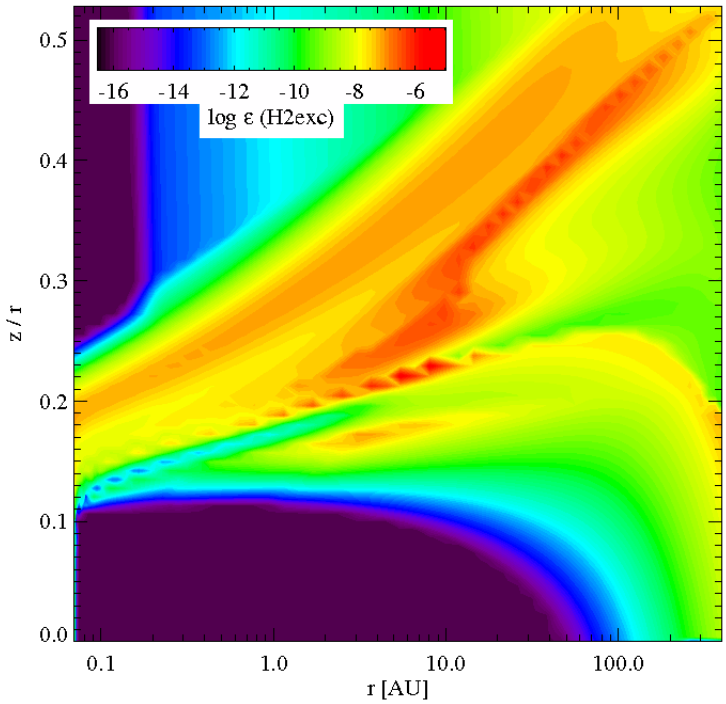

Figure 5: *Excited H_2 in the standard model*

2.2 Reactions of excited H_2

By looking at the reactions that destroy excited H_2, you can see where H_2 influences the chemistry of the disk. Excited H_2 does not always have a large effect on a reaction, it is probably most important for reactions that have an energy barrier or are endothermic. The energy that is required to overcome the potential barrier between the different minima of potential energy of the reactants and the products, is the energy barrier. Endothermicity means that a reaction absorbs energy from the surroundings.

The extra energy that $H_2(v = 1)$ contains, can be used to overcome the activation barrier of a reaction. The first vibrational level contains an extra energy of 0.545 eV with respect to the ground state and this can increase the reaction rate (Tielens and Hollenbach 1985, Hierl et al. 1997).
It might be that not all of the extra energy is available to decrease the activation barrier. The same goes for endothermic reactions, for them, the endothermicity can be decreased, or the reaction can even become exothermic.

Fig. 7 shows the main destruction rates. Again each number indicates a certain reaction, the most important reactions and the number that belongs to them will be discussed here.
One of the ways to destroy excited H_2, is when it returns to the ground state by emitting a photon. This happens at different places in the disk and it is indicated by the number 8. Excited H_2 can also go to the ground state when there is a collision:

$$H_2(v = 1) + H \rightarrow H_2 + H \tag{3}$$

This reaction is important below the surface layer, as shown by number 2. Important reactions in the surface layer are:

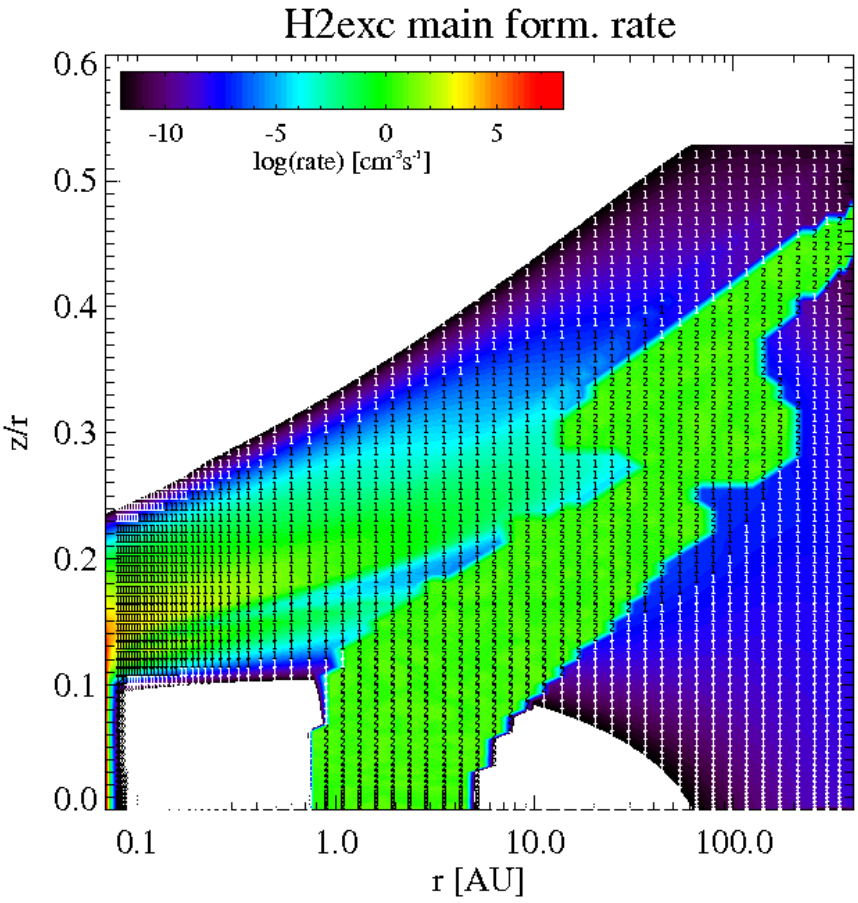

Figure 6: *Formation of excited H_2 in the standard model. The "1" and "2" indicate, that the main formation reaction at that place is respectively reaction (1) or (2)*

$$H_2(v = 1) + H \rightarrow H + H + H \tag{4}$$

$$H_2(v = 1) + He^+ \rightarrow H^+ + H + He \tag{5}$$

The numbers 4 and 12 belong to reaction (4) and (5) respectively. The latter occurs mostly close to the star. Reactions (5) to (9) are listed in Table 3. Reaction (a) is with H_2 in its ground state, reaction (b) with $H_2(v = 1)$.

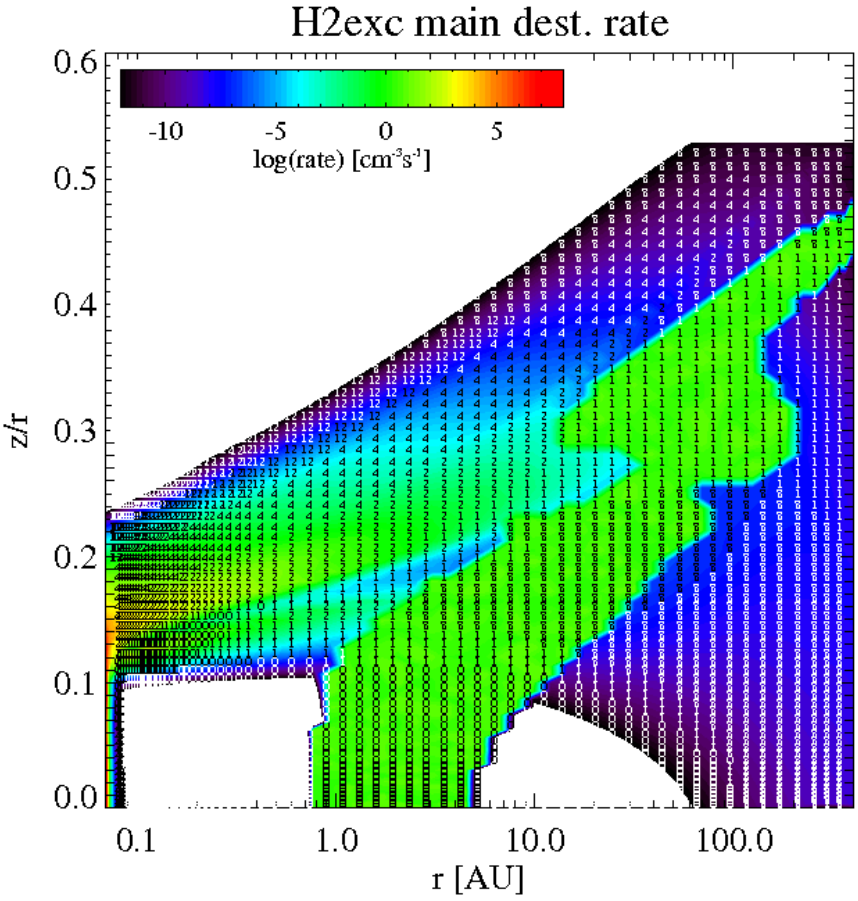

Figure 7: *Destruction of excited H_2 in the standard model. "4" indicates reaction (4), "12" indicates reaction (5)*

Table 3: Reactions of excited H_2

Number	**Reaction**	**A (cm^3 s^{-1})**	**B**	**C**
5a	$H_2 + He^+ \rightarrow H^+ + H + He$	$1.50{\cdot}10^{-13}$	0	0.0
5b	$H_2(v = 1) + He^+ \rightarrow H^+ + H + He$	$0.50{\cdot}10^{-9}$	0	0.0
6a	$H_2 + C^+ \rightarrow CH^+ + H$	$7.80{\cdot}10^{-10}$	0	4537.0
6b	$H_2(v = 1) + C^+ \rightarrow CH^+ + H$	$1.00{\cdot}10^{-8}$	-1.65	0.0
7a	$H_2 + O \rightarrow OH + H$	$9.00{\cdot}10^{-12}$	1.0	4500.0
7b	$H_2(v = 1) + O \rightarrow OH + H$	$3.14{\cdot}10^{-13}$	2.70	0.0
8a	$H_2 + OH \rightarrow H_2O + H$	$8.80{\cdot}10^{-13}$	1.95	1420.0
8b	$H_2(v = 1) + OH \rightarrow H_2O + H$	$2.05{\cdot}10^{-12}$	1.52	0.0
9a	$H_2 + CN \rightarrow HCN + H$	$4.04{\cdot}10^{-13}$	2.87	$8.20{\cdot}10^{2}$
9b	$H_2(v = 1) + CN \rightarrow HCN + H$	$4.04{\cdot}10^{-13}$	2.87	0.0

A, B and C are the A, B and C coefficients for an Arrhenius equation described in Sect. 1.2 and are given for the standard model.

A little deeper into the disk, the following reaction, indicated by number 1, is one of the main destruction reactions:

$$H_2(v = 1) + C^+ \rightarrow CH^+ + H \quad (6)$$

A secondary destruction reaction is:

$$H_2(v = 1) + O \rightarrow OH + H \quad (7)$$

This one is not shown in Fig. 7, it takes place in approximately the same region as reaction (3). But even a secondary destruction reaction can be important.

Agúndez et al. (2010) also discussed reactions of excited H_2 in PDRs. They studied reactions (5), (6) and (7) that were mentioned above. Other reactions where excitation of H_2 might be important are:

$$H_2 + OH \rightarrow H_2O + H \quad (8)$$

$$H_2 + CN \rightarrow HCN + H \quad (9)$$

In these reactions H_2 can be excited or in the ground state. As stated before, the temperature can also have a large influence on the reaciton rates. One of the reactions that depended on temperature was reaction (6). By studying different papers about the reaction rate of that reaction, we found that the rate from the standard model should be changed. The next section discusses the different rates that were used in the papers and in this research.

2.3 Reaction rate for H_2(v=1) + C^+

The initial reaction rate for reaction (6) was determined by an Arrhenius fit to data from Hierl et al. (1997). In Fig. 8 a plot of the data with the reaction rate that is used in the standard model in ProDiMo is shown. The horizontal, dashed line represents the constant value that was used by Agúndez et al. (2010). The rate they used was the Langevin collision rate, 1.6 $\cdot 10^{-9} \mathrm{cm}^3\mathrm{s}^{-1}$. This rate is typical for reactions of an ion with a neutral species. Because the rate constant is close to the collision limit, the same rate holds for low temperatures (Agúndez et al. 2010).

For the temperature range where there was data, the rates from ProDiMo and the Langevin collision rate do not differ a lot. For low temperatures however, the rate in ProDiMo gets much larger than the constant value. The reaction rate in ProDiMo depends on temperature, but since the data from Hierl et al (1997) does not cover low temperatures, it is difficult to say which value should be used.

In a recent paper of Zanchet et al. (2013b) a double Arrhenius equation with a switching function was used to fit their calculated points. This approach was chosen because a single Arrhenius equation was insufficient to fit a wide range of temperatures. They used an exact quantum time dependent method to derive the reaction rate (Zanchet et al. 2013a) Their rate looked like this:

$$k(T) = f^+\alpha_1(T/300)^{\beta_1}\exp(-\gamma_1/T) + f^-\alpha_2(T/300)^{\beta_2}\exp(-\gamma_2/T)$$

Where $f^{\pm}$ is the switching function that lets the two Arrhenius equations combine smoothly. $f^{\pm} = 1/2 + 1/2 \tanh(\pm a(b\text{-}T))$

The parameters for different rotational and vibrational levels can be found in Table 3 from Zanchet et al. (2013b). For the reaction where H_2 is in its first vibrational excited state and

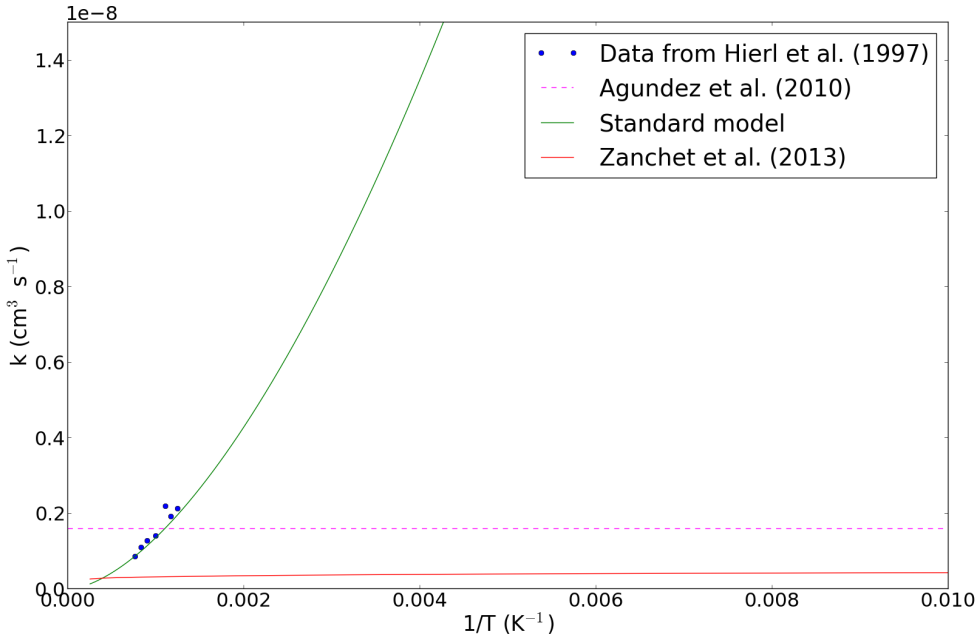

Figure 8: *Different reaction rates*

its rotational ground state (v=1, j=0), the parameters are :
a = 4.314e-5, b = 1432.5,
$\alpha_1 = 7.417 \cdot 10^{-10}$, $\alpha_2 = 1.7164 \cdot 10^{-10}$,
β_1 = -0.151, β_2 = -0.114
$\gamma_1 = 5.936$ and $\gamma_2 = 1724.09$.
Their temperature dependence is less than first was assumed in ProDiMo. The second part adjusts the rate for higher temperatures. Fig. 8 shows that the fit from Zanchet et al. (2013) is lower than the values calculated by Hierl et al. (1997), because they used their own data. It is also more than a factor three smaller than the Langevin collision rate, adopted by Agúndez et al. (2010). Compared to the reaction rate of the standard model, it almost looks like a straight line, but Fig. 9 is zoomed in more and here the temperature dependence is clear.

Since the reaction rate from Zanchet et al. (2013b) differs so much from the original rate in the standard model in ProDiMo, we decided to adjust the rate. Only three coefficients can be given in ProDiMo, so a fit of a single Arrhenius equation to the double one used by Zanchet et al. (2013) was necessary. The result is shown in Fig. 9.

The values for A, B and C from an Arrhenius equation are: $3.88 \cdot 10^{-10}$, -0.136 and -4.242 respectively. Because C is negative, the power of the exponent is positive. The value for C means that as the temperature gets lower, the reaction rate does not keep increasing. At about 50 K the rate will drop. This new rate was used in three of the models.

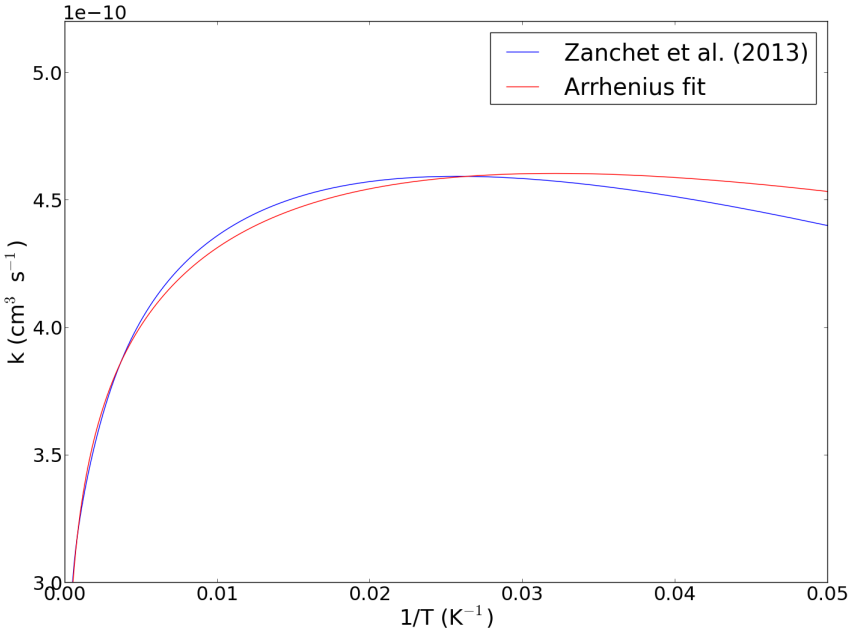

Figure 9: *Single Arrhenius equation fitted to Zanchet et al. (2013)*

3 Comparison of physical quantities

Agúndez et al. (2010) noted that for the reaction with excited H_2 to become important, it should be competitive with respect to the reaction that occurs when H_2 is in the ground state. By competitive is meant that the reaction with excited H_2 should not occur much less than the one with H_2 in the ground state. If that condition does not hold, it means that the reaction with excited H_2 contributes only a small fraction when it is compared to how often the reaction takes place when all states of H_2 are taken into account. The reaction with excited H_2 should also be competitive with respect to other reactions that use the other reactant. If the reactant reacts a lot more with other species than excited H_2, the latter does not make a large difference for the amount of the product. The abundance of excited H_2 relative to that of the ground state and the rate enhancement compared to the reaction rate with H_2 in the ground state both play a role in how competitive the reaction is. If the relative abundance of excited H_2 is very high, the rate enhancement can be small, and the reaction with $H_2(v = 1)$ can still be competitive with respect to the one with $H_2(v = 0)$.
The other way around is also possible. If other reactions consume the species with which $H_2(v = 1)$ reacts and they are much more efficient than the reaction with $H_2(v = 1)$, the latter does not influence the chemistry of the disk significantly. Therefore, both conditions should hold.

Table 4: Parameters of the models

Model	**H_2(v = 1)**	**Reaction rate**	**Star type**	**fUV**
Model 1	yes	normal	T Tauri	0.01
Model 2	no	-	T Tauri	0.01
Model 3	yes	adjusted	T Tauri	0.01
Model 4	yes	adjusted	T Tauri	0.5
Model 5	yes	adjusted	Herbig Ae/Be	0.01

We compared a couple of models, they are listed in Table 4. The first model is the standard one, described before, with a hundred species, that are listed in Table 2.
In the second model, excited H_2 was removed, so 99 species remained. All other parameters stayed the same.
In the adjusted rate model, the reaction rate for the following reaction was modified to match more recent data.

$$H_2(v = 1) + C^+ \rightarrow CH^+ + H$$

The model in which this rate was changed had all other parameters the same as the standard model.

Another model was one that had an increased UV flux. In Sect. 2 it was said that fUV was 0.01 in the standard model, this was increased to fUV = 0.5 and pUV = -1.5. The extra part of UV radiation that was added to the model, would not intercept with the blackbody spectrum if pUV stayed the same as in the standard model. In this model, the adjusted rate reaction (6) was also used. In reality it could be that stars have a higher UV excess than was assumed in the standard model, that is why we were interested in what changes there are if fUV is changed.

The last model we looked at was a disk around a Herbig Ae/Be star. A Herbig Ae/Be star was chosen, because there are observations (Thi et al. 2011, Fedele et al. 2013) of this type of star, so we could compare our model with these observations. This type of stars has a larger mass and higher total luminosity than were used before. The properties used for this model were: $M = 2.2\ M_\odot$, $T_{eff} = 10500$ K and $L = 27\ L_\odot$. It had the adjusted reaction rate for reaction (6).

In the first three models the radiative transfer results were frozen just as the gas temperature. This means that only the amount of excited H_2 or the reaction rate was changed. In the last two models, radiative transfer and gas temperature could not be frozen, because then the extra radiation could not have any influence on the disk chemistry.

To compare the five models, we investigated the images generated by ProDiMo. The masses of different species in the different models were also compared. They can be found in Table 5.

Table 5: Masses of several species in all the models.

Species	**Standard model** ($M_\odot$)	**Model without** $H_2(v=1)$ ($M_\odot$)	**Adjusted rate model** ($M_\odot$)	**Model fUV = 0.5** ($M_\odot$)	**Herbig Ae/Be star** ($M_\odot$)
$H_2(v=1)$	4.4e-11	-	1.2e-10	1.1e-9	3.5e-10
He	2.8e-3	2.8e-3	2.8e-3	2.8e-3	2.8e-3
CH^+	4.7e-14	1.8e-15	1.5e-14	1.8e-13	9.6e-14
OH	1.8e-10	1.7e-10	1.7e-10	7.5e-10	3.5e-10
H_2O	6.0e-8	6.0e-8	6.0e-8	8.0e-8	1.7e-7
HCN	3.9e-10	3.9e-10	3.9e-10	5.0e-10	1.1e-9
CH_2^+	4.7e-14	4.3e-14	4.6e-14	1.1e-13	8.5e-14
CH_3^+	1.5e-12	1.1e-12	1.1e-12	3.0e-12	2.4e-12
HCO^+	7.5e-13	3.1e-13	3.1e-13	7.0e-13	7.0e-13

3.1 Excited H_2

To begin with, it is interesting to look how the amount of excited H_2 changes in the models, because this can tell something about how much is generated by excitation and how much of it reacted with other species. The models .
The model with the adjusted reaction rate has more excited H_2 than the standard model. This is explained by the fact that the reaction rate is lower, so less excited H_2 will react with C^+ to form CH^+. This caused the mass of excited H_2 to be almost a factor of three higher than in the standard model. The amount of CH^+ should decrease in this model, if the former reasoning is correct.
In the fourth model, with an increased UV flux, the mass is much higher, but this time not only because of the reaction rate, but also because the UV excites H_2. Fig. 5 can be compared to Fig. 10 to see that there is more excited H_2 in the second image.
In the model with a Herbig Ae/Be star, there is also more excited H_2 than in the standard model and the adjusted rate model. The star is hotter than the standard star, so more H_2 can be excited, but apparently the increased UV flux for a T Tauro star, is more efficient than the overall luminosity increase to excite H_2.

3.2 CH^+

The first reaction where excited H_2 seems to play an important role, is reaction:

$$H_2(v=1) + C^+ \rightarrow CH^+ + H \tag{6}$$

This reaction is endothermic by 0.374 eV for ground state H_2 (Gerlich et al. 1987). When it is in the first vibrational state, the reaction becomes exothermic. We assumed that all the extra energy of the excitation can be used in overcoming the endothermicity, so it would become exothermic by 0.171 eV.

The formation reactions of CH^+ are shown in Fig. 11. Reaction (6) is indicated by the number 14. This reaction is the most important in the upper part of the disk, at radii larger than 10 AU. The area flares out as you move to a larger radius. In the region where most

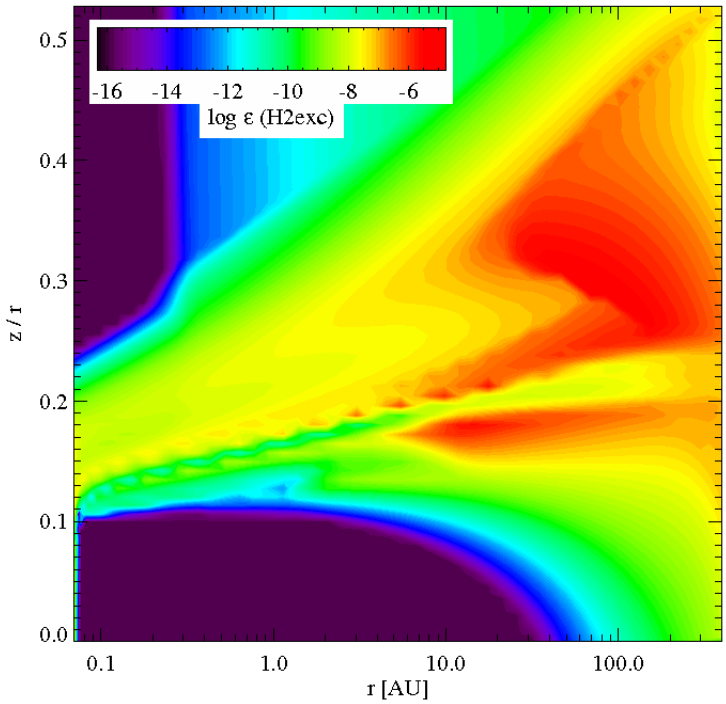

Figure 10: *Excited H_2 in the model with fUV = 0.5*

formation takes place, reaction (6) is second most important, together with for example:

$$H_2 + C^+ \rightarrow CH^+ + H \tag{10}$$

This is denoted by 6. In the surface layer, the reaction indicated by 13 is very important:

$$H + C^+ \rightarrow CH^+ + \text{photon} \tag{11}$$

Comparing this to the result from the model without excited H_2, shows us that reaction (6) has been replaced by reaction (11), which is indicated by 15 in Fig. 12. Also reaction (10) is a little more important in some places. The number 8 indicates this reaction.

The figure also shows that there is less formation of CH^+ if there is no excited H_2 present. Since there is less formation, there is probably also less mass of CH^+. Of course, this is not necessarily true, since the destruction rate could be lower as well. But excited H_2 does not directly destruct CH^+ and the destruction rates do not change a lot. In Fig. 13 the amount of CH^+ in the first two models is shown.

Proof for this is given in Table 5, were the mass of CH^+ can be found. The mass dropped by more than an order of magnitude in the model without excited H_2.
From this can be concluded that excited H_2 is important for the formation of CH^+.

When the reaction rate is adjusted, there is less CH^+, this was already predicted in Sect. 3.1. The difference is a little more than a factor three. This corresponds to the difference in mass of excited H_2.

When the UV flux is higher, the amount of CH^+ is also much higher than before. It in-

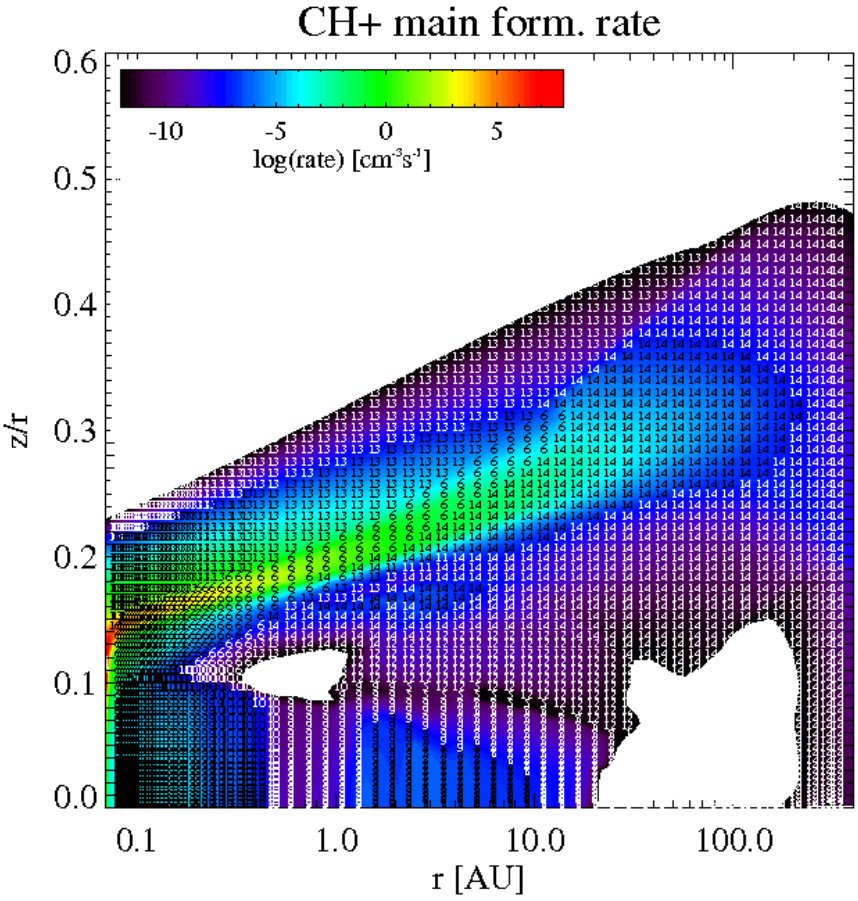

Figure 11: *Formation of* CH^+ *in the standard model. Number "14" indicates reaction (6), "6" is for reaction (10), "13" is for reaction (11).*

creased by more than an order of magnitude with respect to the adjusted rate model. The amount of excited H_2 was also higher in this model, so there is again a correlation between both species.
In the Herbig Ae/Be star there is more CH^+ than in the standard and the adjusted rate model. CH^+ still follows the same trend as excited H_2.

Overall, there is a correlation between CH^+ and excited H_2. Because of the adjusted reaction rate, excited H_2 will have less influence on CH^+, but the models show that excited H_2 is still important.

3.3 He

Another promising reaction seemed to be reaction:

$$H_2(v = 1) + He^+ \rightarrow H^+ + H + He \tag{5}$$

This was one of the main destruction reactions of excited H_2, so it should have an effect on excited H_2. Table 5 however shows that there is no difference in mass when the models are compared. This indicates that the reaction of He^+ with $H_2(v = 1)$ does not hold the first

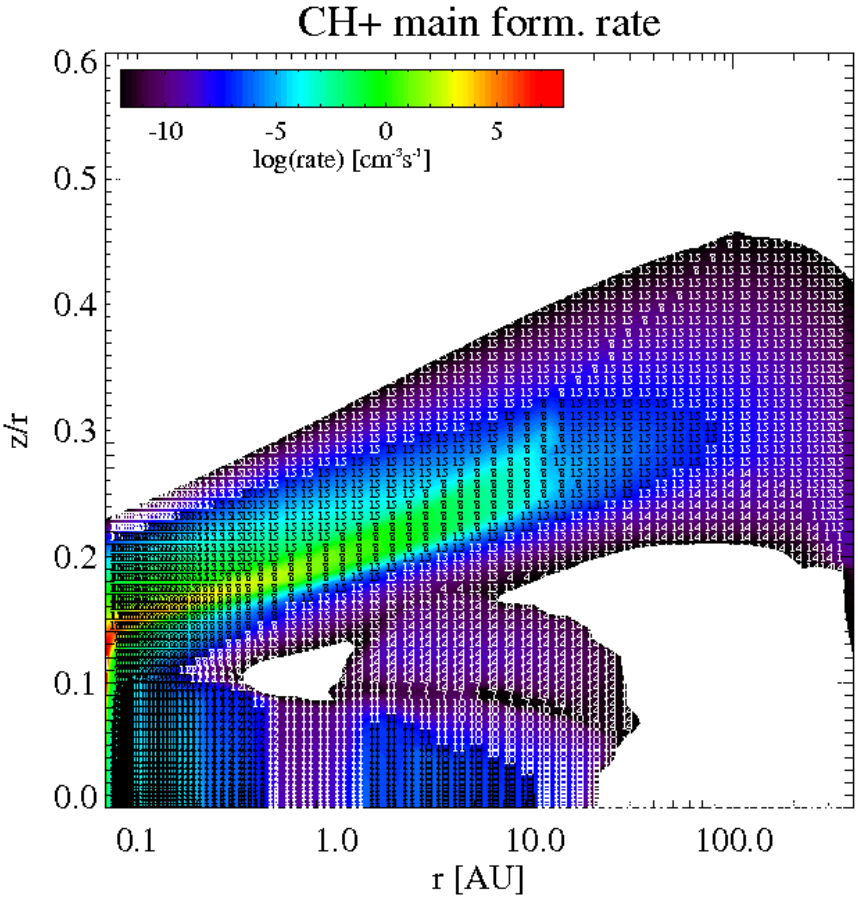

Figure 12: *Formation of CH^+ in the model without $H_2(v = 1)$. Number "15" indicates reaction (11), "8" indicates reaction (10).*

criterium stated by Agúndez et al. (2010). It is not competitive with the reaction that uses $H_2(v = 0)$.
This is because the rate enhancement is not large and a lot of excited H_2 is needed to let it become important for the formation of He (Agúndez et al. 2010). The mass of He is eight orders of magnitude larger than that of excited H_2, which makes it very hard for excited H_2 to play an important role. The other models show the same, since the mass stays the same in all of them.

3.4 OH

The following reaction was another interesting one to look at:

$$H_2(v = 1) + O \rightarrow OH + H \tag{7}$$

It is endothermic by 0.08 eV and has an activation barrier that is 0.4 eV (Agúndez et al. 2010).

Fig. 14 shows the abundance of OH in the standard model, the one without excited H_2 and the model with fUV = 0.5. There is less OH in the surface layer, where the reaction of O with excited H_2 was most prominent. The mass of OH decreased somewhat in the model that had no

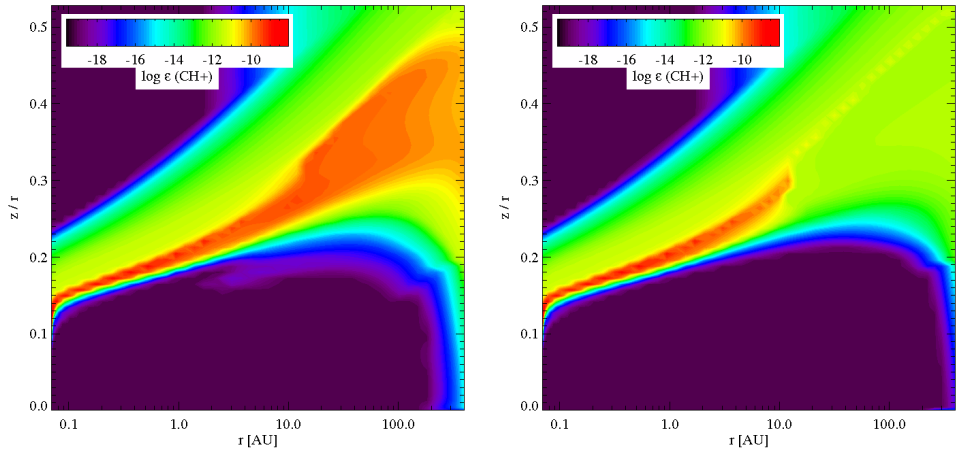

Figure 13: *Left: CH^+ in the standard model. Right: CH^+ in the model without $H_2(v = 1)$*

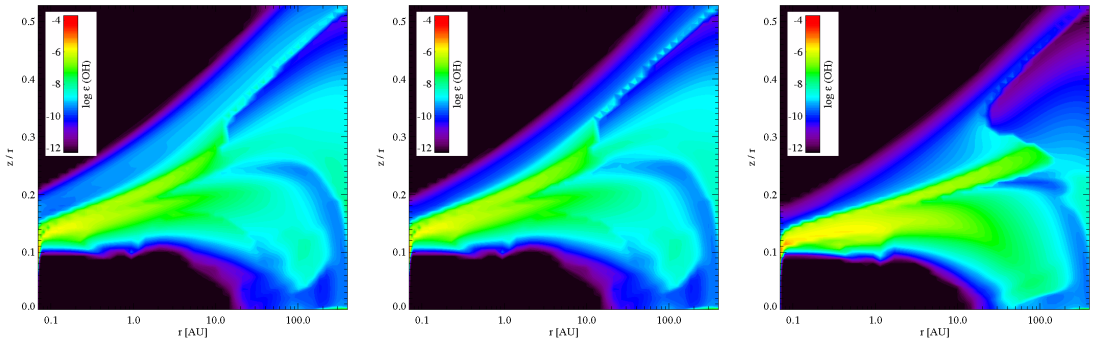

Figure 14: *Left: OH in the standard model. Middle: OH in the model without $H_2(v = 1)$. Right: OH in the model fUV = 0.5.*

excited H_2, it went from $1.8 \cdot 10^{-10}$ $M_\odot$ in the standard model to $1.7 \cdot 10^{-10}$ $M_\odot$. Reaction (7) was most important in the surface layer of the disk, another important reaction in that region was:

$$H_2 + O \rightarrow OH + H \tag{12}$$

Since reaction (7) was only important at a place that already had a low formation rate of OH in the surface layer, the removal of excited H_2 does not have a large influence on the mass of OH. In the model with fUV = 0.5, there is more OH, as can be seen in Fig. 14 in image on the right. The change in OH was largest in this model. This is not only because there is more excited H_2, it is mostly because of the reaction:

$$H_2O + \text{photon} \rightarrow OH + H \tag{13}$$

The places where OH is located partly changed in this model. Excited H_2 does not have a large influence on OH, because the extra OH is not in the regions where excited H_2 increased.

The mass of OH in the last model is in between the fUV = 0.5 model and the other three models. Since the mass of OH did not change a lot in the first three models the conclusion for OH is that radiation has more effect on OH than excited H_2.

3.5 H_2O

One of the ways to form H_2O is through a reaction with excited H_2. This is reaction:

$$H_2 + OH \rightarrow H_2O + H \tag{8}$$

Since most excited H_2 is in the surface layer and that is the place where reaction (8) is one of the main formation reactions for H_2O, it is very well possible that H_2O becomes less abundant in the second model.

When looking at the amount of H_2O in both models however, only a small difference is visible. This can be seen in Fig. 15.

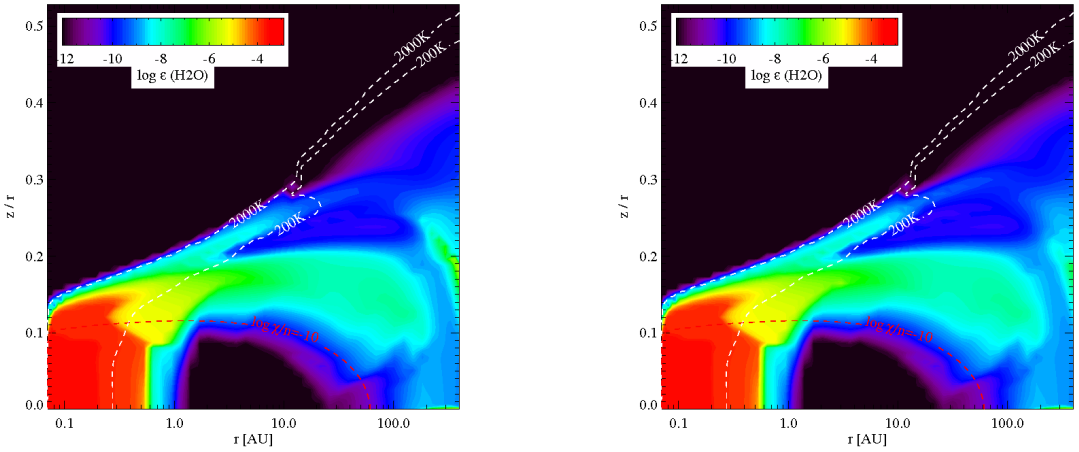

Figure 15: *Left: H_2O in the standard model. Right: H_2O in the model without $H_2(v = 1)$. White dashed lines are isotherms, the red dashed line gives log(χ/n)=-10. χ is the interstellar radiation field, n is the total number density of hydrogen.*

In the surface layer, the main formation reaction changed from the reaction (8) to the reaction of H_2 in its ground state with OH and the radiative association reaction:

$$H + OH \rightarrow H_2O + \text{photon} \tag{14}$$

The mass of H_2O barely changed, so excited H_2 does not influence the mass of H_2O. In the last two models, the amount of H_2O did increase, especially in the Herbig star model. But since the presence or absence of excited H_2 had no effect, the extra radiation in the last two models is responsible for the increase in mass. The reaction of excited H_2 did not influence H_2O.

3.6 HCO^+

The masses of most species did not change a lot when excited H_2 was removed. One of the species that did have a noticable change of mass though was HCO^+. In the standard model there was $7.5 \cdot 10^{-13}$ $M_\odot$ of it and this was decreased to $3.1 \cdot 10^{-13}$ $M_\odot$ in the model without excited H_2.
Fig. 16 shows how much HCO^+ both models have and where it is located. Because the change is only a factor 2.5 and the figures have a logarithmic scale, the change is hard to see in these figures.

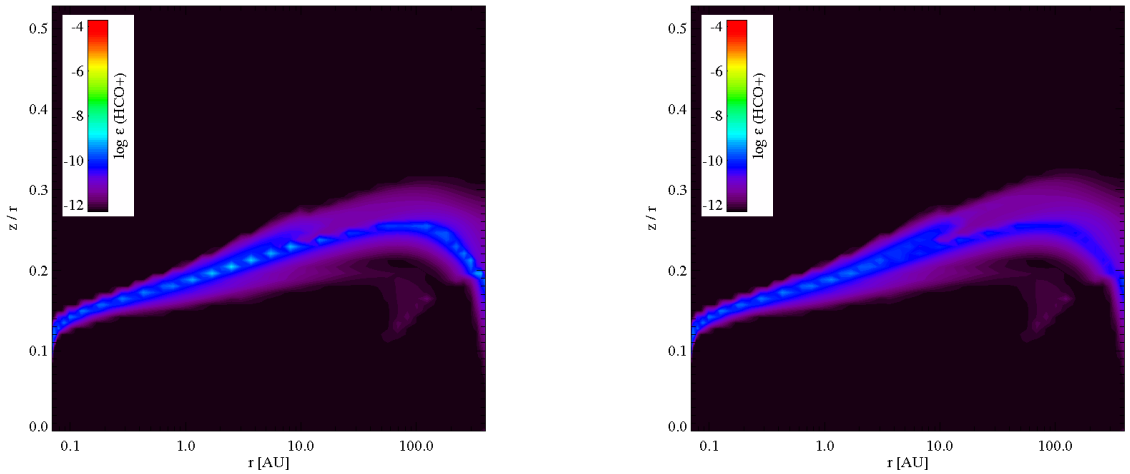

Figure 16: *Left: HCO^+ in the standard model. Right: HCO^+ in the model without $H_2(v = 1)$.*

No direct reaction of excited H_2 with another species to form HCO^+ occurs in the disk, but through a chain of reactions, excited H_2 is important for the formation of HCO^+.
This chain starts when CH^+ is being formed. CH^+ can react with H_2 to form CH_2^+ and this can again react with H_2 to form CH_3^+. Through this exothermic reactions, the abundances of CH_2^+ and CH_3^+ are strongly related to that of CH^+ (Agúndez et al. 2010).

These reactions are indirectly influenced by the presence of excited H_2:

$$CH^+ + H_2O \rightarrow HCO^+ + H_2 \tag{15}$$

$$CH_2^+ + O \rightarrow HCO^+ + H \tag{16}$$

$$CH_3^+ + O \rightarrow HCO^+ + H_2 \tag{17}$$

None of them is the main formation reaction in a large region, but they are important enough to have a detectable effect on HCO^+. Most HCO^+ is concentrated in one layer below the surface. In the centre of this layer, the abundance of HCO^+ decreased a little for the second model. That also happened to the abundance of CH^+.

The third model, with the adjusted reaction rate, also shows the dependence of HCO^+ on CH^+. There is less CH^+ because reaction (6) is less efficient and this causes the mass of HCO^+ to decrease as well with respect to the first model. The mass is just slightly more than in the second model.

When the mass of CH^+ increases in the model with fUV = 0.5, the same happens for the mass of HCO^+, but the latter did not increase as much as the mass of CH^+. This could be because HCO^+ is also formed by reactions that do not depend indirectly on excited H_2, such as:

$$C^+ + H_2O \rightarrow HCO^+ + H \tag{18}$$

$$H_3^+ + CO \rightarrow HCO^+ + H_2 \tag{19}$$

For these reactions, the change in mass of excited H_2 and of CH^+ has no influence. Since they are very important for the formation of HCO^+, the mass of HCO^+ changes less than that of CH^+.

The last model of a disk around a Herbig Ae/Be star, shows the same behaviour. There is less HCO^+ than was expected. The reason for this could be the same as for the fUV = 0.5 model.

Through multiple reactions excited H_2 has an impact on HCO^+. But because there are also reactions that form HCO^+, but that do not depend on excited H_2, the mass of HCO^+ changes less than that of CH^+. This means that HCO^+ is influenced by excited H_2, but not as much as CH^+ is influenced by it.

4 Comparison of observable quantities

The properties that were compared in the previous section were only available from a model, but we cannot observe them in reality. How much of the changes that were visible with some of the species would be observable from real protoplanetary disks?
To answer this, one has to know first which quantity can be observed. The line emission that is emitted as a species goes from an excited state to a lower state is very important in observations. For the species that have line emission and were mentioned before, Table 6 shows the flux in different models.

These line fluxes were calculated by using the escape probability (Woitke et al. 2009). This is the probability that a photon at a certain point will indeed escape it's local environment. If it is absorbed again, it will not contribute to the line flux we detect. The escape probability is not equal to the pumping probability in protoplanetary disks, because starlight is the main source of pumping and these probabilities are only equal with isotropic background radiation (Woitke at al. 2009).

If the mass of a certain species changed, but this happened close to the opaque midplane, there will probably be not a lot of difference in the line flux. At the same time, the mass can change only a little, but if this happens at the surface layer, it might be possible to see a change in flux. A line can be optically thick, in this case not all of the line flux can be observed. The observed flux will thus be lower than the flux would be if all of the emission could be observed. So, the amount of a species has an influence on the strength of the flux that is emitted, but it is not always a one-to-one relation.

4.1 CH^+

The five lines shown in Table 6 all decreased in flux when the excited H_2 was removed. They correspond to the transitions: J = 6-5, J = 5-4, J = 4-3, J = 3-2 and J = 2-1 from top to bottom. The one at 179.6 microns even decreased by more than an order of magnitude. This was $8.3{\cdot}10^{-21}$ W/m^2 in the standard model and went to only $4.7{\cdot}10^{-22}$ W/m^2 in the second model. When the reaction rate was adjusted, the line flux of all the lines decreased with respect to the standard model, but were still slightly higher than in the model without excited H_2. The line at 179.6 microns became much stronger. The line at 179.6 microns is the line from J = 2-1, so the CH^+ is in a low rotationally excited state. It seems that as the lines come from higher exitational levels, the influence of excited H_2 is less.
If CH^+ is formed in the rotational ground state, it can go to a rotational excited state by collisions. The distribution of CH^+ over the rotational energy levels should follow a Boltzmann distribution. The lower levels have a higher population than the higher ones. The distribution over the levels is exponential, so not all levels will increase in population by the same amount. The low levels will increase more than the high ones. This is why the increase in flux of the lines from low rotational levels should be more than that of high levels. More about the Boltzmann distribution is in Sect. 4.4.

The mass of CH^+ in the adjusted rate model decreased a factor three compared to the standard model, but the line fluxes changed less than a factor three. This indicates that the lines are optically thick. Some of the emission is blocked by the CH^+ that is above it, thus it cannot be observed.
In the model with fUV = 0.5, all fluxes increased by approximately two orders of magnitude. A star that emits more UV radiation will cause the surroundings to receive more radiation,

Table 6: Line fluxes of several species in the standard model and the model without excited H_2.

Species	**Wavelength (μm)**	**Standard model (10^{-18} W/m^2)**	**Model without H_2(v = 1) (10^{-18} W/m^2)**	**Adjusted rate model (10^{-18} W/m^2)**	**Model fUV = 0.5 (10^{-18} W/m^2)**	**Herbig Ae/Be star (10^{-18} W/m^2)**
CH^+	60.24	4.4e-3	3.8e-3	3.9e-3	0.26	0.20
CH^+	72.14	8.9e-3	5.1e-3	6.1e-3	0.67	0.63
CH^+	90.01	1.0e-2	3.6e-3	6.0e-3	0.77	0.73
CH^+	119.85	9.7e-3	1.6e-3	5.7e-3	0.62	0.53
CH^+	179.59	8.3e-3	4.7e-4	5.7e-3	0.33	0.23
OH	71.22	1.8	1.9	1.9	55	36
OH	71.17	1.7	1.8	1.8	47	32
OH	79.12	1.7	1.7	1.7	30	27
OH	79.18	1.7	1.7	1.7	31	28
OH	119.23	3.2	3.3	3.3	56	45
OH	119.44	3.6	3.7	3.7	68	51
o $-$ H_2O	538.29	0.40	0.36	0.36	0.57	0.36
o $-$ H_2O	179.52	2.0	1.9	1.9	5.4	4.8
p $-$ H_2O	89.99	1.6	1.6	1.6	12	8.0
o $-$ H_2O	78.74	1.3	1.4	1.4	15	9.8
o $-$ H_2O	63.32	0.62	0.65	0.64	15	7.4
p $-$ H_2O	269.27	1.5	1.4	1.4	2.8	2.1
p $-$ H_2O	187.11	0.13	0.13	0.13	1.6	0.64
HCN	1127.52	5.4e-2	5.3e-2	5.3e-2	0.12	3.8e-2
HCN	845.66	8.89e-2	8.7e-2	8.7e-2	0.27	7.7e-2
HCO^+	3361.33	5.8e-5	2.3e-5	2.3e-5	3.4e-5	3.4e-5
HCO^+	1120.48	4.2e-3	1.7e-3	1.7e-3	4.1e-3	4.2e-3
HCO^+	840.38	6.9e-3	2.9e-3	2.0e-3	1.0e-2	1.0e-2

The strength of the flux is calculated for a distance of 140 parsec.

thereby exciting it. When a species falls back to a lower state, it will emit radiation.
In the case of CH^+, the volume averaged gas temperature is important for the increase in flux. In Kamp et al. (2011), the calculation of this volume averaged gas temperature is given as:

$$<T_g^{sp}> = m_{sp}/M_{sp} \int (n_{sp}(r,z)\ T_g(r,z)\ dV)$$

m_{sp} is the species mass, n_{sp} its density, M_{sp} is the total mass of the species. The average gas temperature for CH^+ is higher than in the previous models, it is 375 K in the fUV = 0.5 model, while it was between 50 and 80 K in the standard and the adjusted rate model. In the fUV = 0.5 model, the gas temperature was not frozen, this affects the population of the rotational levels.
In the Herbig Ae/Be star model, there was less CH^+ than in the fUV = 0.5 model, but the fluxes did not decrease that much. The star used in this model has a higher temperature and emits more radiation. The average gas temperature for CH^+ was 441 K, so it is again higher than when the gas temperature was frozen. This causes a different level population than before.

4.2 OH and H_2O

The amount of both OH and H_2O did not change a lot in all models and the line fluxes also show no large changes. The o-H_2O lines are the ortho-H_2O states, where the nuclear spins of the H atoms are in the same direction. In the para-H_2O, these nuclear spins are antiparallel. All lines of OH increased in flux when fUV = 0.5, because the average gas temperature for OH increased in this model. This was mainly not due to excited H_2. For H_2O the average gas temperature also increased in this model. The same happens for the Herbig Ae/Be star model, only the increase in flux is somewhat less than with fUV = 0.5.

4.3 HCO^+

All shown line fluxes from HCO^+ in Table 6 decreased in the second model when compared to the standard model. They were more than two times as small in the model without excited H_2. The fluxes in the model with the adjusted rate are almost the same as in the second model. The increase is less than the increase in flux of CH^+ from the second to the third model.
For the model with fUV = 0.5, the increase for that of HCO^+ is small compared to the change there was in flux with CH^+. The mass of HCO^+ also changed less than was expected for this model, that could be the reason for the small change in flux. It is the same for the model with the Herbig Ae/Be star.

4.4 Boltzmann plots

The Boltzmann distribution describes the distribution of populations over different excitation states of a system. In the case of CH^+ it describes how much of it is in which energy level. The Boltzmann equation can be used to calculate level populations if collisional coupling is high. This means that excitation comes mainly from collisions and not from, for example, pumping by high-energy photons. Boltzmann plots, also known as rotational plots, can show if the lines are from a region in local thermal equilibrium (LTE) and if they are optically thin. If these conditions hold, a Boltzmann plot shows a straight line. The gas temperature can be derived from such a plot, if it is known where the emission comes from and if the lines come from the same region.

In these plot, the natural logarithm of the column density is plotted against the energy. Goldsmith and Langer (1999) show by going through the following steps how such a plot can give the rotational temperature. For a Boltzmann distribution the column density goes like:

$$\frac{N_j}{N_i} = \frac{g_j}{g_i} e^{-(E_j - E_i)/kT}$$

If the species is in LTE, the population for a single level can be calculated by using the partition function, $Z = \sum_{\text{all levels}} N_i$ and:

$$N_u = \frac{N}{Z} g_u e^{-E_u/kT}$$

where N_u is the column density of the upper level, N the total column denisty, Z the partition function, g_u the statistical weight of the upper level, E_u the energy of the upper level, k the Boltzmann constant and T the rotational temperature.
Taking the natural logarithm on both sides gives:

$$ln(N_u) \propto -E_u/kT$$

When plotting $ln(N_u)$ against E_u and energy is given in Kelvin, the slope gives the rotational temperature of the species. The Boltzmann constant has units of energy per Kelvin, so when energy is given in Kelvin, it is actually the energy divided by the Boltzmann constant. In LTE and if the lines are optically thin, the rotational temperature is the gas temperature. The column density is not something we can directly observe, but it related to the flux:

$$F \propto N_u g_u A_{ul} h \nu_{ul}$$

Where ν_{ul} is the frequency for the transition upper $\rightarrow$ lower level and A_{ul} is the corresponding Einstein A coefficient, g_u the statistical weight and h the Planck constant. The Einstein A coefficients come from the LAMDA database (Schöier et al. 2005). The statistical weight can be calculated by:

$$g_u = 2J_u + 1$$

By using all this information, the Boltzmann plot for CH^+ in the standard model is shown in Fig. 17. The slope is: -0.00789, by taking -1/slope the rotational temperature is calculated, the values for all models are shown in Table 7. Errors on the slope are calculated by omitting the first or the last point of the data from ProDiMo. For the standard model, ignoring the first point results in a lower limit on the rotational temperature. An upper limit on the rotional temperature is given by omitting the last point. This gives T = 127 (+19/-14) K for the standard model. The volume averaged gas temperature for CH^+ gives 55 K. In Sect. 4.1, it was mentioned that the lines for CH^+ are optically thick, this can be the reason that the rotational temperature is not equal to the gas temperature. In Table 8 the gas temperatures of CH^+ in the different models can be found. The rotational temperature is different for the gas temperature for all models.
In the model without excited H_2, the slope is -0.00434 and T = 230 (+10/-3) K, which is a lot higher than in the standard model. The lower limit is derived by omitting the second last point, because omitting the last point gave a higher temperature than was calculated by using all the points. When the second last point was not included, the lowest rotational temperature was derived.

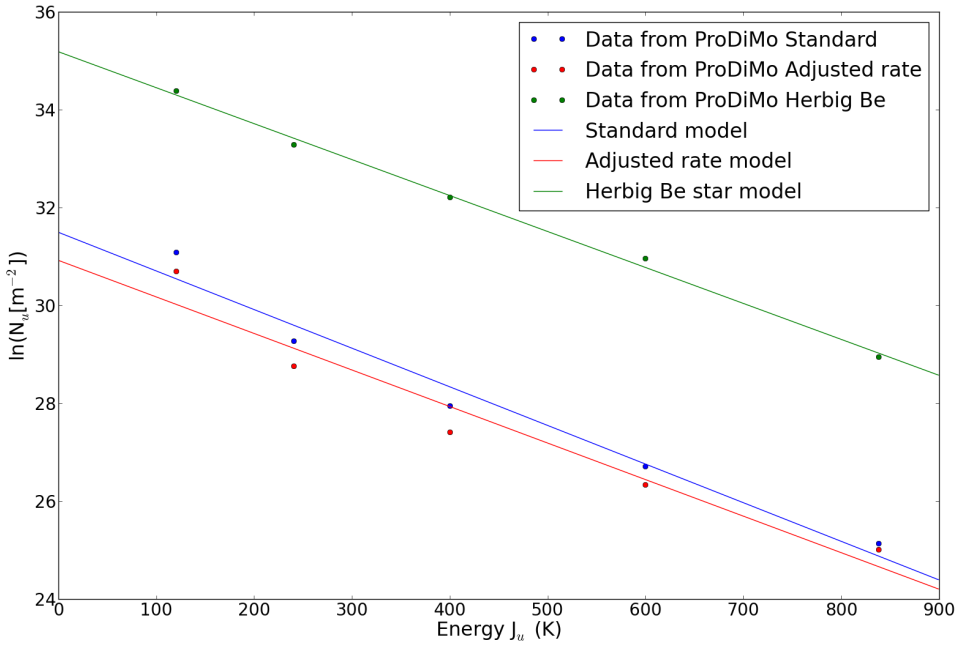

Figure 17: *Boltzmann plot for CH^+. Blue is the standard model, red is the adjusted rate model and green is the Herbig Ae/Be star model*

In the adjusted rate model, a Boltzmann plot gives a rotational temperature of 134 (+29/-20) K since the slope is: -0.00746. The plot is also shown in Fig. 17.
The fUV = 0.5 model gives T = 134 (+9/-3) K.
In the model with the Herbig Ae/Be star, the effective temperature of the star was larger than in all the other models. The emission lines will come from the optimal place in the disk, where the energy is close to the excitation energy. Because this star is hotter, the region where line emission comes from in this model, is farther away from the star than in the standard model. Emission coming from the optimal place also means that the rotational temperature will not change a lot compared with the other models.
This can be seen in the Boltzmann plot that has a slope of -0.00735, which gives: T = 136 (+3/-2) K. The lower limit was again derived by omitting the second last point. Omitting that point gave the lowest temperature.

Table 7: Rotational temperatures

Model	**Rotational temperature (K)**
Standard model	127 (+19/-14)
Model without excited H_2	230 (+10/-3)
Adjusted rate model	134(+29/-20)
Model fUV = 0.5	134 (+9/-3)
Model Herbig Ae/Be star	136 (+3/-2)

Errors are in the brackets

Table 8: Gas temperatures for CH^+

Model	**Gas temperature (K)**
Standard model	55
Model without excited H_2	162
Adjusted rate model	78
Model fUV = 0.5	375
Model Herbig Ae/Be star	441

5 Comparison results from ProDiMo with results from real objects

In the section before the observable quantities of protoplanetary disks were discussed. By comparing the output of a model with observations, it is possible to learn how processes work in real objects. A model should help in understanding the reality. It is useful to compare a model to observations, because this will make clear whether the model is a good approximation of reality or not.

Thi et al. (2011) measured fluxes of CH^+ from a protoplanetary disk around a Herbig Ae/Be star, HD 100546, with the similar properties as the Herbig Ae/Be star model. The object was HD 100546. They had results for four emission lines, although one of them was blended with a line of H_2O. Their fluxes can be found in Table 1 of Thi et al. (2011). When these fluxes are compared with the ones from ProDiMo with the Herbig Ae/Be star model, one can see that the values ProDiMo calculates are two and sometimes almost three orders of magnitude smaller. But HD 100546 is at a distance of about 103 pc (exoplanet.eu/catalog), while the line fluxes from ProDiMo are at a distance of 140 pc. However, this can only explain a factor of approximately 0.54 difference between the fluxes. Another reason for the difference in flux can be that the disk in ProDiMo has an inner radius of 0.1 AU, while the inner radius of HD 100546 is 10 AU. The emission of CH^+ starts at a radius of 2 AU in ProDiMo. For HD 100546, the emission has to start at a larger radius. Thus, the surface area from which the line emission is emitted is larger for HD 100546. This explains why the flux from ProDiMo is less than the observed flux from HD 100546.

In Thi et al. (2011) the rotational temperature for CH^+ was also calculated, they found T = 322 (-151/+2320) K. Their values can be compared to the ones obtained by the last model. The Boltzmann plot for that model is in Fig. 17. The temperature in that model was 136.1 K, which is higher than that of the standard model, but still a lot lower than the value obtained by Thi et al. (2011). It does not fall within the error of 322 -151 K.

Another paper that discusses CH^+ line fluxes and the rotational temperature, is from Fedele et al. (2013). The objects for which they had observed CH^+ line fluxes, were HD 100546 and HD 97048. The first is the same object that Thi et al. (2011) had, the second is a Herbig Ae star, with a mass of 2.5 $M_\odot$ and a luminosity of 40 $L_\odot$. The mass of the star in the Herbig Ae/Be star model is 2.2 $M_\odot$ and L = 27 $L_\odot$, so HD 97048 differs from the model for these parameters.

Table 4 of Fedele et al. (2013) shows the line fluxes for CH^+. All their fluxes for HD 100546 are a little larger than the ones from Thi et al. (2011), except for the one that was blended with an H_2O line in Thi et al. (2011), but they are of the same order of magnitude. The fluxes for HD 97048 are between 2 and 3 $\cdot 10^{-17}$ W m^{-2}. HD 97048 is at a distance of 180 pc, the fluxes should be multiplied by a factor 1.3 before comparing them to the fluxes from the model. The difference with the fluxes calculated by ProDiMo is approximately two orders of magnitude.

A Boltzmann plot for HD 100546 was also made by Fedele et al. (2013), resulting in an excitation temperature of about 80-120 K. This is lower than was calculated by Thi et al. (2011), but closer to the value calculated from ProDiMo. Fedele et al. (2013) had more line fluxes than Thi et al. (2011), this gives a different slope. The difference is slope resulted in the difference in temperature.

6 Conclusion

Five different models were run in ProDiMo to see how excited H_2 would influence other chemical species in a protoplanetary disk. Properties that were changed were the amount of excited H_2 and the reaction rate for reaction:

$$H_2(v = 1) + C^+ \rightarrow CH^+ + H$$

Other properties that varied were the amount of UV excess from the central star and the type of central star. We looked at the plots from ProDiMo with the abundances for different species and at destruction reactions of excited H_2 to see which species changed in the models and may be influenced by the presence of excited H_2. The masses of selected species were compared. Not all of the changes that were detected were caused by excited H_2. The first and the second model were important for knowing whether the change was due to excited H_2 or to other causes, since these models were exactly the same, only the excited H_2 was removed in the second model.

The conclusion was that excited H_2 has most influence on CH^+. The reaction rate for the reaction that forms CH^+ from excited H_2 had to be adjusted, because there was new data (Zanchet et al. 2013) that showed a reaction rate different from the one used before by ProDiMo. The reaction became less efficient than in the standard model, but the amount of CH^+ still depended on the excited H_2. Through a chain of reactions, starting with CH^+, HCO^+ was also dependent on excited H_2. This dependence was less than that of CH^+, since reactions from other species were also important to form HCO^+.

We were also interested in how and if these changes would be observable from real objects. The comparison of masses is something that is possible only because ProDiMo is a model, in reality this has to be derived from observable quatities. For this, the fluxes from emission lines from different models were compared and Boltzmann plots were made. The fluxes from CH^+ in the model without excited H_2 were lower than in the adjusted rate model. The line at 179.6 μm decreased with almost one order of magnitude in the model wihtout excited H_2. Even if the errors of observations, due to for example seeing and sensitivity of the telescope, are taken into account, this difference could be detected. The higher rotational lines showed less difference and it would be difficult to derive from them if there is excited H_2 present. For the lines from HCO^+, the difference was very small. When there are observational errors, this is probably not observable.

The rotational temperature for CH^+ was calculated for different models. For the adjusted rate model the rotational temperature was 134.0 K. All models had temperatures around 130 K, except for the model without excited H_2. That model had T = 230.6 K. This difference in temperatures could be a way to conclude whether excited H_2 is present or not.

The last model that was a disk around a Herbig Ae/Be star. The quantities from this model could be compared to observed results from Thi et al. (2011) and Fedele et al. (2013) for HD 100546. It was found that ProDiMo had much smaller values for the line fluxes from CH^+ than were observed, even if the fluxes were corrected for the distance of HD 100546. The rotation temperature was much smaller than calculated by Thi et al. (2011), pretty close to the one from Fedele et al. (2013)

Further research can be done on how other excited levels of H_2 influence the composition

of protoplanetary disks. A higher vibrational level has more energy and it could be that there is enough energy to overcome activation barriers of other reactions as well. We only looked at a vibrationally excited level, but rotationally excited levels could also be taken into account. The difference in rotational temperature for the model without excited H_2 with respect to the adjusted rate model is also a topic that could be researched. Another topic for research is if ProDiMo also gets lower line fluxes for CH^+ than the typically observed fluxes if the inner radius of the disk is larger and the model is a better represantation of HD 100546.

7 Acknowledgements

I would like to thank Inga Kamp for finding me a research project, for her guidance during the research and explaining various concepts. Also thanks to Rosina Bertelsen for helping me with the Boltzmann plots. Finally, thanks to Anke Arentsen and Jakob van den Eijnden for making our room a pleasant place and sharing experiences.

8 References

Adams, F. C., Lada, C. J., Shu, F. H. (1987) The Astrophysical Journal, Vol. 312, pp. 788-806

Agúndez, M., Goicoechea, J. R., Cernicharo, J., Faure, A., Roueff, E. (2010) The Astrophysical Journal, Vol. 713, pp. 662-670

Aikawa, Y., Herbst, E. (1999) Astronomy and Astrophysics, Vol. 351, pp. 233-246

Andre, P., Ward-Thompson, D., Barsony, M. (1999) in Protostars and Planets IV, University of Arizona Press, pp. 59-96

Bergin, E. A. Aikawa Y., Blake G. A., van Dishoeck E. F. (2007) in Protostars and Planets V, University of Arizona Press, pp.751-766

Calvet, N., Magris, G. C., Patino, A., D'Alessio, P. (1992) Revista Mexicana de Astronomia y Astrofisica, Vol. 24, pp. 27-42

Draine, B. T. (2003) Annual Review of Astronomy and Astrophysics, Vol. 41, pp. 241-289

Dubrulle, B., Morfill, G., and Sterzik, M. (1995) Icarus, Vol. 114, pp. 237-246

Dullemond, C.P., Hollenbach, D., Kamp, I., D'Alessio, P. (2006) in Protostars and Planets V, University of Arizona Press, pp. 555-572

Fedele, D., Bruderer, S., van Dishoeck, E. F., Carr, J., Herczeg, G. J., Salyk, C., Evans, N. J., Bouwman, J., Meeus, G., Henning, Th., Green, J., Najita, J. R., Güdel, M. (2013) Astronomy and Astrophysics, Vol. 559, A 77

Gerlich, D., Disch, R., Scherbarth, S. (1987) The Journal of Chemical Physics, Vol. 87, Issue 1, pp. 350-359

Goldsmith, P. F., Langer, W. D. (1999) The Astrophysical Journal, Vol. 517, pp. 209–225

Habart, E., Walmsley, M., Verstraete, L., Cazaux, S., Maiolino, R., Cox, P., Boulanger, F., Pineau des Forêts, G. (2005) Space science reviews, Vol. 119, pp. 71-91

Hartmann, L., Calvet N., Gullbring E., D'Alessio P. (1998) The Astrophysical Journal, Vol. 495, pp. 385-400

Hierl, P. M., Morris, R. A., Viggiano, A. A. (1997) Journal of Chemical Physics, Vol. 106, pp. 10145-10152

Kamp, I., Woitke, P., Pinte, C., Tilling, I., Thi, W.-F., Menard, F., Duchene, G., Augereau, J.-C. (2011) Astronomy and Astrophysics, Vol. 532, A 85

Kenyon, S. J. and Hartmann, L. (1987) The Astrophysical Journal, Vol. 323, pp. 714-733

Lynden-Bell, D. and Pringle J. E. (1974) Monthly Notices of the Royal Astronomical Society, Vol. 168, pp. 603-637

Muzerolle, J., Calvet, N., Briceño, C., Hartmann, L., Hillenbrand, L. (2000) The Astrophysical Journal, Vol. 535, L47

Rydgren, A. E., Zak, D. S. (1987) Astronomical Society of the Pacific, Publications, Vol. 99, pp. 141-145

Schöier, F. L., van der Tak, F. F. S., van Dishoeck, E. F., Black, J. H. (2005) Astronomy and Astrophysics, Vol. 432, pp. 369-379

Shaw, A. M. (2006) Astrochemistry, from astronomy to astrobiology (John Wiley & Sons Ltd)

Thi, W.-F., Ménard, F., Meeus, G., Martin-Zaïdi, C., Woitke, P., Tatulli, E., Benisty, M., Kamp, I., Pascuccu, I., Pinthe, C., Grady, C. A., Brittain, S., White, G. J., Howard, C. D., Sandell, G., Eiroa, C. (2011) Astronomy and Astrophysics, Vol. 530, L2

Tielens, A. G. G. M., Hollenbach, D. (1985) The Astrophysical Journal, Vol. 291, pp. 722-754

Weidenschilling, S. J. and Cuzzi, J. N. (1993) in Protostars and Planets III, pp. 1031-1060. Eds. E. H. Levy and J. I. Lunine.

Williams, J. P., Cieza, L. A. (2011) Annual Review of Astonomy and Astrophyics, Vol. 49, pp. 67-117

Woitke, P., Kamp, I., Thi, W.-F. (2009) Astronomy and Astrophysics, Vol. 501, Issue 1, pp. 383-406

Zanchet, A., Godard, B., Bulut, N., Roncero, O., Halvick, P., Cernicharo, J., (2013a) The Astrophysical Journal, Vol. 766, pp. 80-88

Zanchet, A., Agúndez, M., Herrero, V. J., Aguado, A., Roncero, O. (2013b) The Astronomical Journal, Vol. 146, Issue 5, pp. 125-132

Sites

http://exoplanet.eu/catalog/hd_100546_b/ (Accessed: 01-07-2014)

http://home.strw.leidenuniv.nl/∼ michiel/ismclass_files/radproc07/chapter8.pdf (Accessed: 01-07-2014)